Galdelli *et al. Journal of Big Data* (2025) 12:115
https://doi.org/10.1186/s40537-025-01163-0

Journal of Big Data

RESEARCH Open Access

Data imputation in large and small-scale spatiotemporal time series gaps using BackForward Bi-LSTM

Alessandro Galdelli[1,2*], Gagan Narang[1], Selene Tomassini[3], Lorenzo D'Agostino[1], Anna Nora Tassetti[2,4] and Adriano Mancini[1]

*Correspondence: a.galdelli@univpm.it

[1] Department of Information Engineering, Università Politecnica delle Marche, Ancona, Italy
[2] National Biodiversity Future Center, Organization, Palermo, Italy
[3] Department of Information Engineering and Computer Science, University of Trento, Trento, Italy
[4] Institute for Marine Biological Resources and Biotechnology, National Research Council, Ancona, Italy

Abstract

In recent years, tracking systems have transformed the understanding of spatiotemporal dynamic processes. However, these systems often face challenges due to missing data caused by technical limitations or intentional manipulation, leading to classification bias and hidden suspicious activities. In response, we propose a deep learning algorithm based on sequential Bidirectional Long Short-Term Memory (BiLSTM) to impute missing trajectories in spatiotemporal datasets. Our approach employs both backward and forward BiLSTMs resulting in BF-BiLSTM architecture to model temporal dependencies before and after the missing trajectories. We evaluated the algorithm on a realistic marine and aerial dataset, considering missing data trajectories on vessels and flights with missing data rates ranging from 5% to 30%. The model improves performance in terms of MAE (0.011°), MSE (0.056%), MAPE (0.054%) and ADE (0.017°) when compared to state-of-the-art approaches. By effectively addressing challenges in spatiotemporal datasets and improving existing benchmarks, our algorithm provides a robust solution for enhancing trajectory imputation in the context of monitoring systems potentially across diverse application domains.

Keywords: Time series, Deep learning, Neural networks, Trajectory imputation, AIS

Introduction

Time series of spatial data are fundamental in physical processes and particularly in scenarios involving continuous monitoring and prediction, such as object tracking. However, unexpected accidents, such as malfunctioned sensors or missing signals, may result in a time series gap and, thus, hamper the use of such data.

Fisheries science and marine ecosystem studies increasingly rely on vessel tracking data, such as Vessel Monitoring Systems (VMS) and Automatic Identification Systems (AIS), which have revolutionized the understanding of spatial and temporal information about fishing activities. These systems generate big data, which is mined to analyze fishing effort patterns and formulate sustainable strategies [1–6]; however gaps in data coverage can occur due to several factors, including technical malfunctions, signal loss, or even intentional interference [7]. In some cases, fishers may deliberately disable their tracking devices, often in attempts to obscure their fishing grounds or engage in illegal fishing activities such as unauthorized fishing in exclusive economic zones and marine protected/fishery-regulated areas or unauthorized transshipments, in which catch from fishing vessels is off-loaded to refrigerated cargo vessels at sea [8–10].

This intermittent absence of data, for instance, as shown in Fig. 1, created from realistic AIS data, where it is not possible to estimate the current position of the vessel, which could also be potentially engaged in illegal fishing activity. This poses a significant challenge in maintaining the integrity of the analysis and hinders the progress of policies aimed at sustainability in the marine environment. Policies such as the Port State Measures Agreement and the European Union's Illegal, Unreported, and Unregulated Regulation depend heavily on accurate and continuous data from tracking systems to enforce fishing regulations and promote sustainable practices [11–13]. Further, it makes such tracking systems inappropriate for absolute estimates of fishing activity and requires advanced methodologies to address the challenge. Some researchers have attempted to mitigate the issue using satellite data and cross-referencing it with AIS data to detect missing vessels [14]. However, this approach struggles with detecting smaller ships and differentiating multiple objects at sea in satellite images, which have been removed to some extent by using multiple sources of image and optimized image processing [15]. Focusing on approaches that improve the reliability of the source AIS data, trajectory imputation is a method that involves estimating missing values based on historical data patterns, and it can be used to reconstruct incomplete trajectories. This ensures the continuity and accuracy of analysis, preventing incomplete data from skewing results. Trajectory imputation can be viewed as a special case of prediction, as it reconstructs missing parts within a known trajectory leveraging the same spatiotemporal dependencies [16].

Efforts have been made in the past regarding trajectory prediction, with major contributions to common pedestrian applications and vehicles on the road. Several researchers have focused on the trajectories that individuals or crowds undertake when walking [17–21]. Among them, Kitani et al. [22] addressed the task of inferring people's

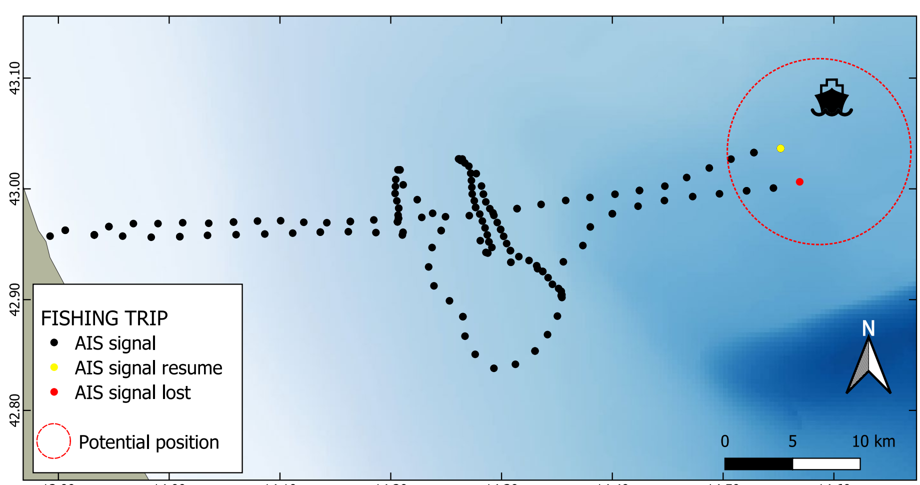

Fig. 1 Gap in AIS signal suggests potential involvement in illegal fishing activities

future actions from noisy visual inputs, Jaipuria et al. [23] presented a novel framework for accurate pedestrian intent prediction at intersections, whereas Huynh et al. [24] proposed a prediction system that incorporated scene information and human-motion trajectories. However, human trajectories mainly depend on environmental/social factors in which they are collected and are mutually influenced by each other [25].

Addressing interpersonal and social aspects of Human-Human Interaction (HHI), Alahi et al. [17] presented the Social-LSTM architecture, whereas Peng et al. [26] introduced a transformer-based multi-person pose forecasting via modeling body part interactions. Gupta et al.'s contribution [18], instead, involved a pooling mechanism and generative adversarial networks for producing socially acceptable trajectories.

The above-mentioned works are specifically designed for human trajectory and HHI prediction. Nevertheless, several methodologies have been proposed for applications in automotive, aircraft, and naval scenarios where prediction presents additional challenges (e.g., large vessel size, higher speeds that increase the likelihood of errors, and network outages [27]). For example, Deep Learning (DL) and adaptive composite frameworks have been incorporated with promising results into understanding the dynamics of road vehicle trajectory [28]. However, trajectory prediction, especially in maritime settings, often lacks access to sufficient datasets, particularly when addressing missing data. Moreover, many existing approaches tend to focus on filling small gaps rather than the more complex task of predicting vessel trajectories during extended blackout periods. In the case of longer gaps, for instance, features such as correlation within the variables of the available dataset through approaches such as Multicollinearity Applied Stepwise Stochastic imputation presented promising results [16]. Nevertheless, it is noted that their application is limited to multidimensional data, which is more common in road transportation than in marine environments.

Compared to human or road vehicle spaces, naval and aerial trajectory prediction involves unique challenges, such as unconstrained motion pathways, which are not definitive as compared to a network of roads. Additionally, more extensive data loss occurs over long distances due to weak network availabilities in challenging marine environments [29]. Therefore, though we have observed considerable improvements and promising results in human or on-road trajectories through georeferencing and satellites, the developed research may not be directly applicable to vessel trajectory imputation problems. In this context, we propose a novel sequential algorithm based on Bidirectional Long Short-Term Memory (BiLSTM) to impute missing vessel trajectories based on previous and future AIS observations. Unlike other state-of-the-art data imputation strategies based on Machine Learning (ML) or DL models with sparse missing data, the proposed approach is developed to impute both small and large portions of the missing sequential data, i.e., up to 5-30% of individual trips. The core findings of the research described in this paper are:

- The implementation of a novel BackForward Bidirectional Long Short-Term Memory (BF-BiLSTM) model for imputing vessel trajectories during data blackouts. We extend the BiLSTM architecture by introducing separate models for capturing backward and forward temporal dependencies before and after the missing trajectories for data imputation. We conduct the validation of the proposed model,

comparing its performance against well-established imputation methods using standard benchmarks and ablation studies. The model is made publicly available at https://github.com/vrai-group/BF-BiLSTM-imputation-trajectory;
- The demonstration of the model generalization capability, by showcasing its imputation performance on an open access aerial trajectory dataset.

Related works

This section focuses on trajectory forecasting and imputation strategies, identifying advancements in both areas and opportunities for intersection. The examined works rely on historical data for informed predictions, yet they differ in their primary objectives, with trajectory forecasting focusing on predicting future positions and data imputation on filling gaps to ensure data completeness.

Trajectory forecasting

Several methods, mostly based on mathematical interpolation, have been proposed since VMS was introduced by the European Union in 2002 to bolster fishery control and enforcement [30], and related datasets were made available only in one-hour or two-hour sampling intervals. Such prolonged polling interval indeed obscures specific trajectory segments between sampled endpoints, thus hampering historical fishing effort distribution analysis [31]. Recently, the integration of ML and DL architectures with data mining has solved many issues related to vessel trajectory prediction during blackout periods and path planning. Zhang et al., in their investigation, found that AIS is the most prevalent and accessible data source, with DL techniques like LSTM dominating. in the forecasting applications [32]. The survey is based on 57 papers of existing research in vessel trajectory prediction, categorizing them into simulation, statistical, ML, DL, and hybrid methods. The study found several state-of-the-art time series forecasting methods for vessel trajectory, based on architectures such as Recurrent Neural Networks (RNNs), Convolutional Neural Networks (CNNs), and more recently, transformers are emerging for missing values and data imputation strategies.

Hintzen et al. [33] adopted the Hermite Cubic Spline to estimate the movement path between two consecutive VMS data points using vessel speed and heading to define an expected trajectory, increase data resolution and in turn improve estimates of the spatial and temporal patterns of trawling activity. This was implemented in the *vmstools R* package [34] and well established by the International Council for the Exploration of the Sea (ICES) related data call. In the same years, Russo et al. equipped their *VMSbase* package [35] with a modification of the Catmull-Rom algorithm to take into account for the different aspects involved in vessel navigation, such as the combined actions of human control and drift by sea current and wind (if present) [36]. Both these techniques rely on mathematical regression to create smooth interpolated curves and lack precision in capturing sharp turns in trajectory segments, introducing errors when interpolating the intricate operational states of trawler fishing trajectories. Addressing this, Zhao et al. [37] introduced a DL approach that, specifically for trawlers, integrates ResNet, LSTM, and multilayer neural network to precisely refine the sampling interval of historical VMS datasets from two hours to just three minutes by harnessing both VMS and marine hydrological datasets. Further, hybrid models as proposed in Magnussen et al. [38] used interpolation schema based on Cubic Hermite Spline and LSTM neural network, applying the model to trawl vessels.

For anomaly detection, Pallotta et al. in [39] and [40] presented the Traffic Route Extraction and Anomaly Detection methodology to classify vessels into routes and predict trajectories along these routes using Ornstein-Uhlenbeck stochastic processes. It is effective for medium and long-term predictions (hours) but unsuitable for short-term collision avoidance (5 to 30 min). Mazzarella et al. in [41] used historical AIS data to present a Bayesian vessel prediction algorithm based on a particle filter, improving vessel position prediction quality. Like Pallotta et al., this algorithm is limited to long-term predictions. Hexeberg et al. in [42] used a single-point neighbour search method to estimate future positions at every prediction time based on historical AIS data, suitable for short-term prediction only (a few minutes up to 15 min).

Imputation strategies

Imputation strategies handle missing values by deletion of instances and replacement with potential or estimated values, and are divided into simple, regression-based, hot-deck, and expectation maximization [43]. The non-missing values data set is usually employed to predict the values used to replace the missing data. Although it addresses different data processing needs, trajectory prediction exhibits a reliance on historical data, and ignoring missing data without imputation impacts the overall assessment application [44]. Towards this, there has been a growing interest in application of DL techniques, with RNNs being the most employed, followed by Gated Recurrent Units (GRUs) and Generative Adversarial Networks (GANs). Though GAN-based generative methods are emerging (e.g., TemporalGAN [45]), the performance isn't a huge upgrade where, generative models compromise on the explainability of the results since they involve complex architectures with probabilistic processes that obscure the decision-making pathways during imputation and, therefore, are frequently used in denoising or pre-processing the datasets more often rather than imputation [46, 47].

LSTM-based models have consistently obtained lower errors in transfer learning application studies as well [48, 49]. Recently, Transformer-based architectures have gained significant attention for their ability to handle long-term dependencies more effectively than RNNs and LSTMs. The self-attention mechanism in transformers allows for better modeling of relationships within the data, making them particularly suited for tasks involving sequential information. Transformer based approaches such as Seq2Seq have gained prevalence; however, they have lagged in long-term prediction tasks [50]. In this context, our research builds on these advancements by introducing a novel BF-BiLSTM model, designed specifically for trajectory imputation in both short-term and long-term data gaps. We compare our model against the best-performing methods, including LSTM-based and Transformer-based models, and demonstrate its performance in handling data gaps at different intervals of missing data.

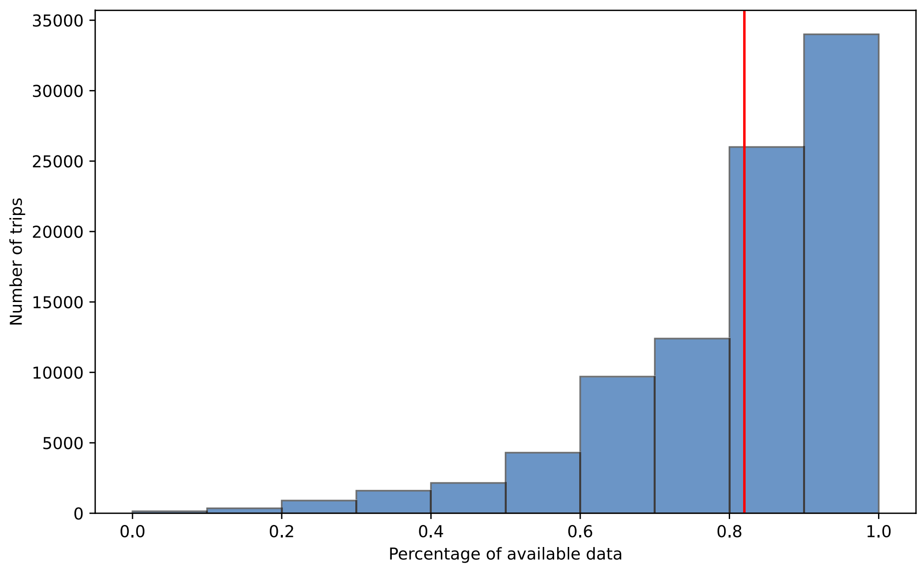

Fig. 2 Number of trips by percentage of available data (Red = average value)

Materials and methods

Dataset

Evaluating imputation methods in complex environments, such as in marine or aerial settings, requires access to realistic trajectory data. We use two datasets; the AIS data used for primary investigation and the TrajAir dataset used for generalization tests.

AIS dataset

Our primary marine dataset, which comprises a high-density collection of AIS data representing 554 renowned Mediterranean vessels and typical to this region, are of fishing activities using different types of gear. Acquired from a private provider,[1] this dataset spans from 2015 to 2018, with temporal updates at five-minute intervals. Although the dataset is privately acquired, a portion of it has already been made publicly available for validation purposes [51], and the performance of our model is also demonstrated on this public subset. Specifically, there are a total of 89,872 trips representing fishing activity supplemented by an indexing table that includes: i) the IDs of the beginning and ending AIS records for each fishing trip; and ii) the temporal duration of the trip. The collected AIS data underwent processing to remove outliers and were resampled to a five-minute poll rate. Collected vessel trips have varying percentages of available and conversely missing data (Fig. 2), with over 33,000 trips with a 90-100% AIS data availability rate, followed by over 25,000 sessions with an 80-90% availability rate.

For training our data imputation method, we use trips with a 100% availability rate. Given the diverse time duration of fishing trips and the average duration of one day, we set a maximum threshold of 5 days. Filtering trips with a maximum duration of 5 days and 100% records yielded 5,571 fishing trips. Due to the variable lengths

[1] www.astrapaging.com.

of each fishing trip, we adopt the shortest one - which lasts 7 h or comprises 84 AIS data points - as the baseline to break down longer sessions into shorter sub-sessions.

Artificial 2-hour blackouts are introduced into each fishing trip. This ensures a subsection of the trajectory serves as ground truth during evaluation. Subsequently, the trained model can be deployed to impute trajectories, even in scenarios where fishing trips exhibit missing data that range from 5 to 30% of overall fishing vessel activities. To evaluate our model's performance and compare with popular existing imputation approaches, and visualize the processing differences, we apply two distinct approaches. Each fishing trip is segmented into 48 points. For prediction models like LSTM, CNN-LSTM, and GRU networks, the initial 24 points for training and predicts the subsequent 24 points. However, our BF-BiLSTM network leveraged the first and last 12 points to predict the 24 central points. The last 12 points in each sub-trip are reversed, and the 24 central points are used as ground truth during evaluation. For visual comparisons, all models are plotted using a consistent selection of forward and backward trajectory segments to ensure comparability. An analysis of AIS data variance identifies sub-sessions associated with stationary vessels, which are subsequently eliminated.

TrajAir dataset

After the performance evaluations on the AIS dataset, to demonstrate the model's adaptability beyond marine applications, we use the TrajAir dataset to test its performance on aerial trajectories. It is a publicly available dataset of aerial trajectories [52]. The dataset provides 111 days of flight data (September 2020-April 2021) around Pittsburgh-Butler Regional Airport (Pennsylvania, USA), including weather information sourced from METAR strings. The data is collected using an on-site Automatic Dependent Surveillance-Broadcast (ADS-B) receiver, which are the equivalent of AIS in the aviation domain. To ensure consistency, we preprocess the data similar to the AIS data, removing outliers and resampling records to match a five-minute interval. Additionally, the weather information available in the dataset was not used, and we focused on imputing spatiotemporal trajectory time series.

Trajectory imputation

The data imputation involves replacing missing data with predicted values based on observed values in preceding and subsequent time steps (Fig. 3). Within this framework, each trajectory position information tuple u is constructed by concatenating a sequence of AIS data parameters, such as Maritime Mobile Service Identity (MMSI), timestamp, latitude, and longitude. We define a singular trajectory point tuple information as:

$$u = MMSI, t, \lambda, \phi, \theta, s \tag{1}$$

where $MMSI$ designates the unique identifier for a vessel's AIS transceiver, t represents the timestamp of AIS transmission, λ and ϕ are the latitude and longitude respectively in WGS84, θ is the Course Over Ground (COG) and s is the Speed Over Ground (SOG). Each element u_k represents the kinematic characteristics, i.e., properties of a vessel's motion, at instant k on the trajectory S. Eventually, n spatially distributed AIS pings

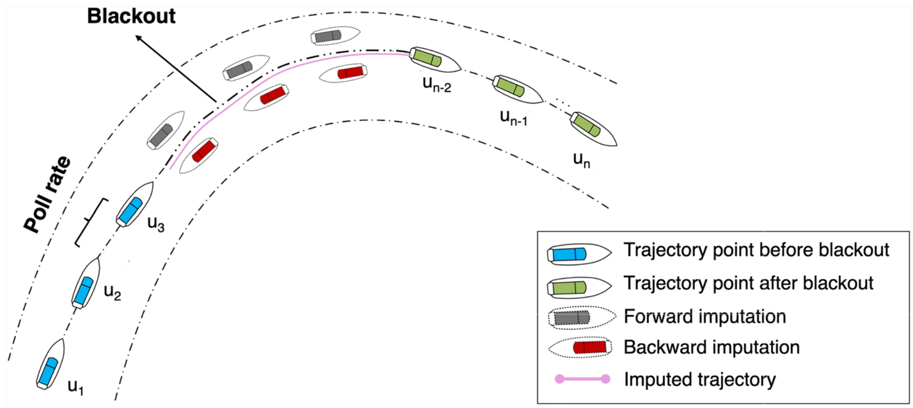

Fig. 3 A sample vessel trajectory imputation illustration

represent each fishing trip according to a fixed transmission period represented by the term 'poll rate'. This rate dictates the frequency of AIS data transmissions, influencing the temporal resolution of the trajectory imputation process. Our data imputation operation is based on latitude, longitude, and time since vessel speed s can be derived using these three variables. Therefore, we redefine the trip as:

$$S = (U(t, \lambda, \phi), T) \tag{2}$$

where S defines a spatiotemporal fishing trip trajectory, U is a set of temporally-ordered sequences of tuple u defined in Eq. 1, T is a set of timestamps of AIS transmission, and $U = \{u_k | k = 1, ..., T_i\}$ with T_i indicating the number of AIS data points comprising the trajectory.

The model learns from the prepared historical trajectories the spatiotemporal mapping of each fishing trip to impute the intermediate missing trajectory segment, denoted as Y_M, with an imputation horizon ranging from 5 to 30% of the total trajectory. Defining T as the temporal duration of the fishing trip, we can represent n as,

$$n = \frac{T}{poll\ rate\ AIS\ data} \tag{3}$$

and then the fishing trip F is defined as,

$$F = \{u_i | i \in [1, 2, ..., n]\} \tag{4}$$

The proposed method should be able to impute trajectories in the short (poll rate AIS data resolution) and long term, minimizing the error (length of Y_M ranges from 5 to 30% of the total trajectories), under the following condition between two consecutive data points:

$$(t_{u_{i+1}} - t_{u_i}) > t_{poll\ rate\ AIS\ data} \tag{5}$$

Addressing the need for continuity in the accuracy of maritime tracking data, we employ two parallel networks: a forward prediction network (P_f) and a backward prediction network (P_g). The forward network P_f is responsible for estimating future trajectory segments, represented as $\overrightarrow{\hat{Y}}_M$, based on historical AIS data leading up to the blackout. Conversely, the backward network P_g aims to reconstruct past trajectory segments denoted as $\overleftarrow{\hat{Y}}_M$, utilizing data available after the blackout period. If t_{gap} denotes the duration of the blackout period, we framed the data imputation problem as:

$$\begin{aligned} \overrightarrow{\hat{Y}}_M &= P_f(u_1, u_2, ..., u_t) \\ \overleftarrow{\hat{Y}}_M &= P_g(u_m, u_{m+1}, ..., u_n) \quad \text{where } m = t + t_{\text{gap}} \end{aligned} \tag{6}$$

The output of forward $\overrightarrow{\hat{Y}}_M$ and backward $\overleftarrow{\hat{Y}}_M$ are concatenated for computing the final imputation $\hat{Y}$. Assuming $\overrightarrow{\hat{Y}}_M$ be approximately equal to u_m, u_{m+1},...,u_n and $\overleftarrow{\hat{Y}}_M$ be approximately equal to u_1, u_2,...,u_t, we obtain the consistency constraints as,

$$\begin{aligned} \hat{Y} &\approx P_f(P_g(u_m, u_{m+1}, ..., u_n)), \\ \tilde{Y} &\approx P_g(P_f(u_1, u_2, ..., u_t)). \end{aligned} \tag{7}$$

In the absence of blackout periods, the problem definition converges to the constraints defined in Eq. 7.

BackForward BiLSTM Architecture

LSTM is a variant of RNN that can learn long-term dependencies through its memory unit, being particularly suited for problems that require searching for patterns in a time series. For the data imputation problem, a single LSTM does not allow us to obtain satisfactory results as they are designated for unimodal prediction problems. In light of this, we implement BF-BiLSTM to successfully impute vessel trajectory during the blackout period, training both forward and backward prediction networks. Figure 4 displays the BF-BiLSTM architecture, which is designed to handle the complexities of trajectory imputation by leveraging bidirectional temporal dependencies. The architecture processes segments of the trajectory through forward and backward BiLSTM layers, integrating these outputs to enhance prediction accuracy.

Let h^f and h^b represent the forward and backward hidden states of the BiLSTM, where:

$$\begin{aligned} h_i^f &= \sigma(W_f h_{i-1}^f + U_f u_i + b_f) \qquad \text{where } 1 \le i \le t \\ h_k^b &= \sigma(W_b h_{k+1}^b + U_b u_k + b_b) \quad \text{where } m \le k \le n \end{aligned} \tag{8}$$

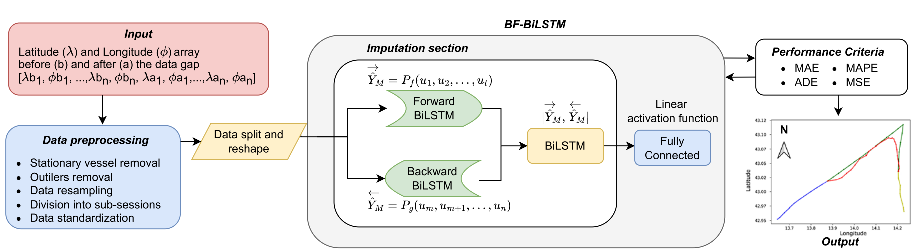

Fig. 4 Proposed BackForward BiLSTM architecture

where, W_f and W_b are weight matrices for the forward and backward BiLSTMs respectively; h^f_{i-1} and h^b_{k+1} are the hidden states at previous and next time steps; U_f, U_b are the input weight matrices; u_i and u_k are the input vectors at time i and k, respectively; σ is the sigmoid activation function; b_f and b_b are the bias vectors for the forward and backward passes. The final hidden state at each time step is obtained by concatenating the forward and backward hidden states:

$$h = [h^f, h^b] \tag{9}$$

Considering the output from Eq. 6, $\overrightarrow{\hat{Y}}_M$ and $\overleftarrow{\hat{Y}}_M$ are then concatenated to form the complete imputed trajectory:

$$\hat{Y} = [\overrightarrow{\hat{Y}}_M, \overleftarrow{\hat{Y}}_M] \tag{10}$$

The final imputed trajectory $\hat{Y}$ is passed through a dense (fully connected) layer with a linear activation function to map it to the correct spatial dimensions (latitude, longitude) and minimize the imputation error.

This bidirectional approach allows the model to utilize information from both past and future data points, providing a comprehensive understanding of the trajectory patterns. The proposed architecture includes an AIS-based sub-trip as input, with the model trained to impute central data. Latitude and longitude values undergo normalization to facilitate training efficiency and generalization across datasets, recognizing that this process should not affect the vessel's 2D path on the sea surface. Several preprocessing steps (i.e., outlier removal, vessel separation, division into sub-sessions, and standardization) ensure the model receives clean and normalized input data, enhancing its performance. The BF-BiLSTM architecture incorporates separate forward and backward BiLSTM layers that process the initial and final segments of the trajectory, respectively, and allow the model to combine contextual information from both directions. These outputs are then merged via concatenation before feeding another BiLSTM layer. This additional layer integrates the bidirectional information more deeply, allowing the model to refine its understanding and improve imputation accuracy. The final layer features a fully connected layer using Linear activation, and ensures that the imputed trajectory data can be seamlessly integrated into existing tracking systems, providing accurate and reliable predictions.

Experiments

The processing of the AIS dataset is presented as a benchmark for assessing our method, followed by the tests conducted to evaluate different DL solutions in terms of imputation performance. All experiments are performed using a GPU NVIDIA® Quadro RTX 6000 with 48 GB of RAM, and the Keras library built on a Tensorflow back-end.

Experimental settings and evaluation parameters

The data is split, using 80% of the total sub-sessions for training and the remaining 20% for testing. The AIS dataset for training is normalized using the *MinMaxScaler* [53] from Scikit-Learn libraries and passed to the networks in a vectorized form:

Table 1 Hyperparameters used to train BF-BiLSTM

Parameter	Value
Optimizer	*Adam*
Learning rate	0.001
Epochs	1500
Batch size	64
Loss	$\frac{1}{n}\sum_{i=1}^{n}\lvert y_i - y_{p_i}\rvert$

$[\lambda_1, \phi_1, \lambda_2, \phi_2, \ldots, \lambda_n, \phi_n]$. In the validation set, the model hyperparameters (Table 1) are tuned and used to train BF-BiLSTM. Further, standard benchmarking metrics [50, 54] were evaluated on each respective test dataset. The evaluation metrics aggregate the errors across both latitude and longitude into a single value, providing a measure of how closely the imputed trajectories match the actual paths. The evaluation metrics can be interpreted as described below:

- *Mean Absolute Error (MAE)* Indicates the average magnitude of the absolute errors, offering a direct measure of error amount without considering direction, i.e., positive or negative. A smaller MAE value indicates that, on average, the imputed geographic points are closer to the actual positions, reflecting higher accuracy. A lower MAE means that the model is performing well in reconstructing vessel trajectories with minimal spatial deviation.
- *Average Deviation Error (ADE)* It reflects the average deviation of the imputed positions from the true coordinates. A lower ADE indicates that the imputed trajectory follows the actual path closely, with minimal deviations. This metric gives an indication of the model's precision.
- *Mean Absolute Percentage Error (MAPE)* It provides a relative measure of accuracy, expressing the error as a percentage of the actual values. The smaller the MAPE, the more reliable the model is in preserving the spatial characteristics of the actual trajectory.
- *Mean Square Error (MSE)* It provides a way to measure the quality of an estimator by reflecting both the variance and the bias. It is reported as percentage (scaled by a factor of one hundred) for improved readability. A lower MSE indicates that most imputed positions are close to the actual ones and that large errors are infrequent.

Each metric mentioned is assessed by computing its value for individual sub-sessions generated through dataset preprocessing, followed by averaging the results. The data for these calculations is de-normalized, presenting the outcomes in decimal degrees.

Hyperparameter optimization strategy

The performance of BF-BiLSTM is optimized by employing the Adam in conjunction with the Hyperband tuner class for hyperparameter selection. This strategy is based on a random search through adaptive resource allocation and early-stopping - which is comparably efficient in contrast to other popular approaches such as Bayesian optimization

Table 2 Comparison of different imputation models applied to marine vessel data using MAE, ADE, MAPE, and MSE metrics with the standard deviation error

Metric	LSTM	CNN-LSTM	BLSTM	GRU	BF-BiLSTM	BRITS	NRTSI	Seq2Seq
MAE [°] (↓)	0.077±0.041	0.037±0.030	0.027±0.028	0.027±0.030	**0.011±0.014**	0.049±0.040	0.031±0.025	0.071±0.039
ADE [°] (↓)	0.123±0.065	0.058±0.048	0.043± 0.045	0.044±0.047	**0.017±0.022**	0.074±0.065	0.046±0.041	0.113±0.062
MAPE [%] (↓)	0.392±0.239	0.183±0.157	0.135± 0.147	0.137±0.158	**0.054±0.069**	0.112±0.068	0.501±0.423	0.353±0.234
MSE [%] (↓)	1.103±1.434	0.361±0.744	0.271± 0.808	0.287±1.220	**0.056±0.526**	0.312±0.208	1.258±1.607	0.970±1.390

Bold values indicate the best-performing model for each metric

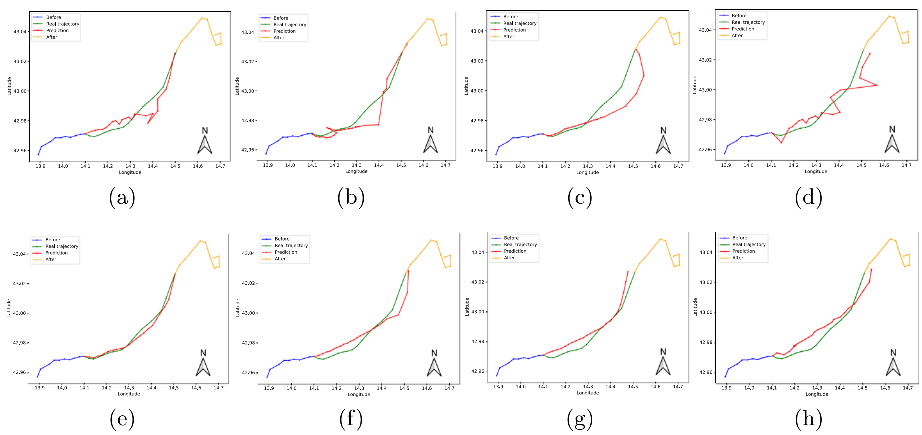

Fig. 5 Illustration of trajectory imputation across models: LSTM (**a**), CNN-LSTM (**b**), BLSTM (**c**), GRU (**d**), BF-BiLSTM (**e**), BRITS (**f**), NRTSI (**g**), and Seq2Seq (**h**) (X-axis = Longitude; Y-axis = Latitude)

[55] - and aims to identify the most effective combination for enhancing model training dynamics and accuracy.

The hyperparameters are chosen, looking for a compromise between quick convergence and accurate model generalization (Table 1). They include learning rate and batch size, with the former tested at values of 0.01, 0.001, and 0.0001 and the latter at 32, 64, 128, and 256. The training duration is set at 1,500 epochs to ensure comprehensive learning. Such optimization minimizes the MAE, thereby narrowing the discrepancy between predictions and real-world values and bolsters the overall model effectiveness.

Results and discussion

The performance of imputation models is assessed, and notably, although seemingly minor, an error of 0.01° on ADE corresponds to a spatial deviation of approximately 1.11 kms in latitude and slightly less in longitude, depending on the specific location. This discrepancy is due to the inherent complexity in the task, requiring substantial data for accurate imputation in an open environment. Despite these challenges, the trajectories are successfully reconstructed, and a detailed comparison is presented in Fig. 5. Table 2 presents a comprehensive analysis of various AIS data imputation models based on evaluation metrics. Among the considered models i.e., LSTM, CNN-LSTM, BLSTM, GRU, BF-BiLSTM, BRITS, NRTSI, and Seq2Seq, the general trend observed is that the

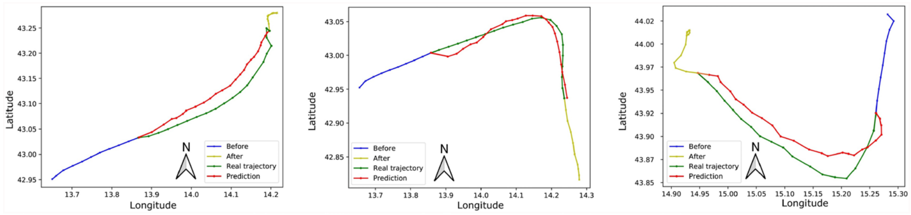

Fig. 6 Imputation of vessel trajectories, using our AIS test dataset

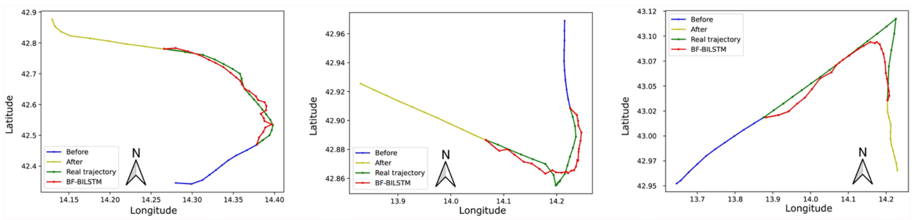

Fig. 7 Imputation of vessel trajectories, using a public validation AIS dataset [51]

BF-BiLSTM model consistently outperforms across the standard metrics. Following the BF-BiLSTM, both BLSTM and GRU exhibit competitive performance.

Specifically, in terms of MAE, the BF-BiLSTM model outperforms others with a significantly lower error of $0.011 \pm 0.014°$, indicating higher accuracy in trajectory imputation. This corresponds to an average positional deviation of roughly $1,200\ m$, and considering a large data gap of 30% of the data, this highlights the model's ability to impute and align with existing data. Following closely are BLSTM and GRU models with errors of $0.027 \pm 0.028°$ and $0.027 \pm 0.030°$, respectively. Regarding ADE, similar trends are observed, with BF-BiLSTM exhibiting the lowest error of $0.017 \pm 0.022°$, followed by BLSTM and GRU models with errors of $0.043 \pm 0.045°$ and $0.044 \pm 0.047°$, respectively. Continuing the trends in MAPE, BF-BiLSTM again stands out with the lowest error of $0.054 \pm 0.069°$, showcasing its effectiveness in maintaining accuracy across diverse scenarios. BLSTM and GRU models follow with relatively higher errors of 0.135 ± 0.147 °and $0.137 \pm 0.158°$, respectively, with BRITS offering lower margins of error at $0.112 \pm 0.001°$. Finally, considering MSE, the BF-BiLSTM model consistently performs well with the lowest error of $0.056 \pm 0.526°$. BLSTM and GRU models also exhibit competitive performance with errors of $0.271 \pm 0.808°$ and $0.287 \pm 1.220°$, respectively.

Generally, the CNN-LSTM network has the lowest performance; this is on account of only two features (latitude and longitude) in the dataset. The optimization obtained by the convolutional layer prevents the network from returning significant results. Further, looking at computational resources, a conventional LSTM underwent training for approximately 50 min using NVIDIA GPU. Despite promising metrics, the model struggled with trajectory predictions due to its simplicity. Similar results were obtained with bidirectional LSTM, GRU, and 1D-convolutional layers. However, these conventional methods fell short of meeting our objectives. The BF-BiLSTM required a longer training time, around 3 h, but delivered superior results.

Figures 6 and 7 depict three instances of imputations by the BF-BiLSTM on different trajectory in our AIS test set and on public validation set, respectively. The collective findings underscore the consistent performance of the BF-BiLSTM model across all metrics, highlighting its robustness in AIS data imputation. Intriguingly, BLSTM and GRU models exhibit competitive performance. Since our model is based on LSTM, we proposed an ablation study of adjusting our model with GRU, resulting in BF-GRU and additional testing on a varying imputation window.

Ablation study

The model is tested with a data imputation window of varying sizes and replacing BiLSTM with GRU modules (to effectively implement the BF-GRU model). This allows us to isolate three key factors: (i) the impact of varying window sizes on imputation accuracy; (ii) the substitution with GRU offers any quantitative or qualitative improvements; (iii) the generalizability of the model to other datasets. The goal is to identify the optimal data window that yields the most favorable results and to evaluate how the GRU, which showed promising results in preliminary experiments, performs when integrated into our model's fully connected architecture, allowing for a comparison of different variations and related datasets.

Specifically, we explore conditions with missing data to be imputed i_{imp} with respect to the size of input points a_{after} and output b_{before} data points. This division accounts for three distinct cases (20%, 33%, and 50% of the total imputation percentage), representing both smaller and wider windows. Table 3 compares BF-BiLSTM and BF-GRU performance under varying degrees of missing AIS data. Notably, the best results are obtained at a window size of 60, characterizing higher forward and backward historical data points. For smaller data gaps, the BF-BiLSTM model achieves the lowest MAE and ADE values of $0.005 \pm 0.005°$, indicating high precision. This error translates to an average deviation of approximately 555 ms in latitude and 400 ms in longitude, showcasing the model's capability to reconstruct shorter segments of missing data. As the window size expands, there is a noticeable trend of a slight rise in imputation errors for both models, reflected in increased MAE, ADE, MAPE, and MSE values. However, BF-BiLSTM

Table 3 Comparison of BF-BiLSTM and BF-GRU performance between different missing AIS data windows

	BF-BiLSTM				**BF-GRU**			
Imputation Percentage	**20%**	**33%**	**50%**	**50%**	**20%**	**33%**	**50%**	**50%**
Window size [AIS points]	**60**	**36**	**24**	**48**	**60**	**36**	**24**	**48**
$[a_{\text{after}} - i_{\text{imp}} - b_{\text{before}}]$	24-12-24	12-12-12	6-12-6	12-24-12	24-12-24	12-12-12	6-12-6	12-24-12
MAE [°] (↓)	**0.005±0.005**	0.007±0.008	0.009±0.010	0.011±0.014	**0.006±0.006**	0.009±0.011	0.012±0.015	0.014±0.018
ADE [°] (↓)	**0.005±0.005**	0.008±0.008	0.012±0.015	0.017±0.022	**0.006±0.006**	0.010±0.010	0.014±0.017	0.019±0.023
MAPE [%] (↓)	**0.029±0.031**	0.043±0.046	0.050±0.059	0.054±0.069	**0.031±0.036**	0.046±0.054	0.057±0.071	0.069±0.087
MSE [%] (↓)	**0.012±0.014**	0.028±0.031	0.067±0.183	0.056±0.526	**0.013±0.016**	0.029±0.035	0.071±0.201	0.062±0.557

Bold values represent the best performance between BF-BiLSTM and BF-GRU for different missing data gaps

Table 4 Comparison of BF-BiLSTM and BF-GRU models on aerial flight data using MAE, ADE, MAPE, and MSE metrics with the standard deviation error

Metric	BF-BiLSTM	BF-GRU
MAE [°] (↓)	**0.018±0.021**	0.022±0.028
ADE [°] (↓)	**0.030±0.032**	0.036±0.047
MAPE [%] (↓)	**0.031±0.001**	0.036±0.060
MSE [%] (↓)	**0.125±0.020**	0.219±0.372

Bold values indicate the best-performing model for each metric

consistently maintains a favorable accuracy compared to BF-GRU across these expanding windows. This observation suggests that while more oversized missing data windows pose a challenge for both models, BF-BiLSTM exhibits better resilience and accuracy in trajectory imputation as the complexity of the imputation task increases.

We conducted a generalizability test to assess whether the BF-BiLSTM model's superior performance in AIS-based vessel trajectory imputation extends to different types of trajectory data, specifically aerial trajectories. In the generalizability test, Table 4 showcases that the BF-BiLSTM model consistently outperforms BF-GRU across all metrics, indicating its effectiveness even in airplane trajectory imputation. Specifically, it achieves the lowest values for MAE of $0.018 \pm 0.021°$, ADE of $0.030 \pm 0.032°$, and MAPE of 0.031 ± 0.001 %. For the MSE, BF-BiLSTM achieves 0.125 ± 0.020 % highlighting its accuracy and robustness in efficiently imputing airplane trajectories. However, it's important to note that the BF-GRU model also demonstrates commendable results, particularly considering the complex nature of aerial trajectory data. The execution time for both models is identical, which suggests that the BF-GRU could still be considered a viable alternative, especially in contexts where model simplicity and computational resources are significant considerations.

Unlike typical fusion models, our BF-BiLSTM architecture excels in handling extensive data gaps and varying trajectory patterns by effectively utilizing bidirectional temporal dependencies. The integration of the architectural innovations to LSTM our model has provided a more robust and accurate solution for trajectory imputation for short and long term imputation and generalizes well on additional trajectory datasets advancing beyond the capabilities of traditional BiLSTM and other existing methods like BRITS. This ensures that our model can handle complex and irregular missing data patterns, making it a valuable tool for various real-world applications requiring reliable and continuous data imputation.

Conclusions

Tracking technologies and remote sensing systems are crucial in monitoring various marine/aerial activities and any data loss has an impact on the environment or business prospects, thereby making systems such as AIS mandatory. Regardless, such systems are prone to intentional or accidental data loss. Towards addressing the reliability of such datasets, we presented a novel BF-BiLSTM model that robustly imputes missing sequential trajectory data, outperforming state-of-the-art imputation methods that comparably require more data to model trajectories over temporally large blackout periods.

Considering past and future information, the proposed model allows the imputation of AIS-based vessel trajectories with data gaps between 5-30% of the overall trip, achieving promising performance over short and long terms where other methods may not, and for different gears. Such ability to handle extensive and irregular data gaps is key for important fishery applications, such as precise historical fishing effort distribution analysis from sparse VMS/AIS data or recovering trajectories that have been manually terminated due to illegal fishing. When tested for generalizability on an aircraft trajectory dataset containing 8 months of aircraft trajectories in an untowered terminal airspace, the BF-BiLSTM model consistently demonstrates its adaptability.

Our model operates under the assumption of a 2D path, focusing only on latitude and longitude, which limits its application in contexts where elevation or depth data are important. The model relies on the availability of both historical and future trajectory data, and its accuracy diminishes when large portions of data are missing without sufficient surrounding information. Future work will consider additional features such as speed and course, as well as an improved ablation study of horizon comparison with other approaches, to understand the significance of each model component further.

Acknowledgements
This study has been funded by the National Recovery and Resilience Plan (NRRP), Mission 4 Component 2 Investment 1.4 - Call for tender No. 3138 of 16 December 2021, rectified by Decree no. 3175 of 18 December 2021 of the Italian Ministry of University and Research funded by the European Union - Next Generation EU. Award Number: Project code CN_00000033, Concession Decree No. 1034 of 17 June 2022 adopted by the Italian Ministry of University and Research, Project title "National Biodiversity Future Center".

Author contributions
A.G.: Investigation, Conceptualization, Methodology, Resources, Visualization, Software, Writing-original draft, Writing-review & editing. G. N. and S. T.: Methodology, Visualization, Software, Writing-original draft, Writing- review & editing. L. D.: Conceptualization, Methodology, Resources, Visualization, Software & editing. A. N. T. and A. M.: Writing-review, editing, Supervision & Validation. All authors read and approved the final manuscript.

Data availability
AIS data is owned by CNR-IRBIM, and made available to Università Politecnica delle Marche within the framework of the NBFC. While the complete AIS dataset cannot be publicly released, the test set is made available along with the developed code on GitHub (https://github.com/vrai-group/BF-BiLSTM-imputation-trajectory).

Declarations

Ethics approval and consent to participate
This article does not involve any studies that were conducted on human or animal participants by any of the authors. Not applicable as there were no participants involved in the study.

Competing interests
The authors declare no Competing interests.

Received: 8 November 2024 Accepted: 18 April 2025
Published online: 09 May 2025

References

1. Lambert GI, Jennings S, Hiddink JG, Hintzen NT, Hinz H, Kaiser MJ, et al. Implications of using alternative methods of vessel monitoring system (VMS) data analysis to describe fishing activities and impacts. ICES J Marine Sci. 2012;69(4):682–93. https://doi.org/10.1093/icesjms/fss018.
2. Russo T, D'Andrea L, Parisi A, Martinelli M, Belardinelli A, Boccoli F, et al. Assessing the fishing footprint using data integrated from different tracking devices: issues and opportunities. Ecol Indi. 2016;69:818–27. https://doi.org/10.1016/j.ecolind.2016.04.043.
3. Eigaard OR, Bastardie F, Hintzen NT, Buhl-Mortensen L, Buhl-Mortensen P, Catarino R, et al. The footprint of bottom trawling in European waters: distribution, intensity, and seabed integrity. ICES J Marine Sci. 2016;74(3):847–65. https://doi.org/10.1093/icesjms/fsw194.
4. Ferrà C, Tassetti AN, Grati F, Pellini G, Polidori P, Scarcella G, et al. Mapping change in bottom trawling activity in the Mediterranean Sea through AIS data. Mar Policy. 2018;94:275–81. https://doi.org/10.1016/j.marpol.2017.12.013.

5. Shepperson JL, Hintzen NT, Szostek CL, Bell E, Murray LG, Kaiser MJ. A comparison of VMS and AIS data: the effect of data coverage and vessel position recording frequency on estimates of fishing footprints. ICES J Marine Sci. 2017;75(3):988–98. https://doi.org/10.1093/icesjms/fsx230.
6. Li Z, Liu T, Peng X, Ren J, Liang S. An AIS-based deep learning model for multi-task in the marine industry. Ocean Eng. 2024;293: 116694.
7. Ferrà C, Tassetti AN, Armelloni EN, Galdelli A, Scarcella G, Fabi G. Using AIS to Attempt a Quantitative Evaluation of Unobserved Trawling Activity in the Mediterranean Sea. Front Mar Sci. 2020;7:1036. https://doi.org/10.3389/fmars.2020.580612.
8. Welch H, Clavelle T, White TD, Cimino MA, Osdel JV, Hochberg T, et al. Hot spots of unseen fishing vessels. Sci Adv. 2022;8(44):2109. https://doi.org/10.1126/sciadv.abq2109.
9. Tassetti AN, Ferrà C, Fabi G. Rating the effectiveness of fishery-regulated areas with AIS data. Ocean Coastal Manag. 2019;175:90–7. https://doi.org/10.1016/j.ocecoaman.2019.04.005.
10. Galdelli A, Mancini A, Ferrà C, Tassetti AN. A Synergic Integration of AIS Data and SAR imagery to monitor fisheries and detect suspicious activities. Sensors. 2021. https://doi.org/10.3390/s21082756.
11. Food and Agriculture Organization of the United Nations.: Agreement on Port State Measures (PSMA). https://www.fao.org/iuu-fishing/international-framework/psma/en/. Accessed 23-10-2024.
12. European Commission.: Agreement on Port State Measures to Prevent, Deter and Eliminate Illegal, Unreported and Unregulated Fishing. https://eur-lex.europa.eu/LexUriServ/LexUriServ.do?uri=OJ:L:2011:203:0001:0001:EN:PDF. Accessed 23-10-2024.
13. The Pew Charitable Trusts.: The Port State Measures Agreement: From Intention to Implementation. https://www.pewtrusts.org/en/research-and-analysis/issue-briefs/2018/04/the-port-state-measures-agreement-from-intention-to-implementation. Accessed 23-10-2024
14. Lee YK, Jung HC, Kim K, Jang Y, Ryu JH, Kim SW. Assessment of maritime vessel detection and tracking using integrated SAR Imagery and AIS/V-Pass Data. Ocean Sci J. 2024;59(2):27.
15. Galdelli A, Narang G, Pietrini R, Zazzarini M, Fiorani A, Tassetti AN. Multimodal AI-enhanced ship detection for mapping fishing vessels and informing on suspicious activities Pattern Recognition Letters. 2025;191:15–22. https://doi.org/10.1016/j.patrec.2025.02.022.
16. Leiby BD, Ahner DK. Multicollinearity applied stepwise stochastic imputation: a large dataset imputation through correlation-based regression. J ig Data. 2023;10(1):23.
17. Alahi A, Goel K, Ramanathan V, Robicquet A, Fei-Fei L, Savarese S. Social LSTM: Human Trajectory Prediction in Crowded Spaces. In: 2016 IEEE Conference on Computer Vision and Pattern Recognition (CVPR); 2016. p. 961–971.
18. Gupta A, Johnson J, Fei-Fei L, Savarese S, Alahi A.: Social GAN: Socially Acceptable Trajectories with Generative Adversarial Networks.
19. Lisotto M, Coscia P, Ballan L.: Social and Scene-Aware Trajectory Prediction in Crowded Spaces.
20. Helbing D, Molnár P. Social force model for pedestrian dynamics. Phys Rev E. 1995;51(5):4282–6. https://doi.org/10.1103/physreve.51.4282.
21. Lian J, Ren W, Li L, Zhou Y, Zhou B. Ptp-stgcn: pedestrian trajectory prediction based on a spatio-temporal graph convolutional neural network. Appl Intell. 2023;53(3):2862–78.
22. Kitani KM, Ziebart BD, Bagnell JA, Hebert M. Activity Forecasting. In: Fitzgibbon A, Lazebnik S, Perona P, Sato Y, Schmid C, editors. Computer Vision - ECCV 2012. Springer, Berlin Heidelberg: Berlin, Heidelberg; 2012. p. 201–14.
23. Jaipuria N, Habibi G, How JP. A Transferable Pedestrian Motion Prediction Model for Intersections with Different Geometries.
24. Manh H, Alaghband G. Scene-LSTM: A Model for Human Trajectory Prediction.
25. Paolanti M, Manco D, Pietrini R, Frontoni E. GREEN PATH: an expert system for space planning and design by the generation of human trajectories. Multi Tools Applic. 2024;1:25.
26. Peng X, Mao S, Wu Z. Trajectory-Aware Body Interaction Transformer for Multi-Person Pose Forecasting. In: Proceedings of the IEEE/CVF Conference on Computer Vision and Pattern Recognition; 2023. p. 17121–17130.
27. Ibrahim R, Shafiq MO. Detecting taxi movements using Random Swap clustering and sequential pattern mining. J Big Data. 2019;6(1):39.
28. Shao Q, Piao X, Yao X, Kong Y, Hu Y, Yin B, et al. An adaptive composite time series forecasting model for short-term traffic flow. J Big Data. 2024;11(1):102.
29. Zhang Z, Fan Z, Lv Z, Song X, Shibasaki R. Long-Term Vessel Trajectory Imputation with Physics-Guided Diffusion Probabilistic Model. In: Proceedings of the 30th ACM SIGKDD Conference on Knowledge Discovery and Data Mining; 2024. p. 4398–4407.
30. Campbell MS, Stehfest KM, Votier SC, Hall-Spencer JM. Mapping fisheries for marine spatial planning: Gear-specific vessel monitoring system (VMS), marine conservation and offshore renewable energy. Mar Policy. 2014;45:293–300. https://doi.org/10.1016/j.marpol.2013.09.015.
31. Katara I, Silva A. Mismatch between VMS data temporal resolution and fishing activity time scales. Fish Res. 2017;188:1–5. https://doi.org/10.1016/j.fishres.2016.11.023.
32. Zhang X, Fu X, Xiao Z, Xu H, Qin Z. Vessel trajectory prediction in maritime transportation: Current approaches and beyond. IEEE Trans Intell Trans syst. 2022;11:98.
33. Hintzen NT, Piet GJ, Brunel T. Improved estimation of trawling tracks using cubic Hermite spline interpolation of position registration data. Fish Res. 2010;101(1):108–15. https://doi.org/10.1016/j.fishres.2009.09.014.
34. Hintzen NT, Bastardie F, Beare D, Piet GJ, Ulrich C, Deporte N, et al. VMStools: Open-source software for the processing, analysis and visualisation of fisheries logbook and VMS data. Fish Res. 2012;115–116:31–43. https://doi.org/10.1016/j.fishres.2011.11.007.
35. Russo T, D'Andrea L, Parisi A, Cataudella S. VMSbase: An R-Package for VMS and Logbook Data Management and Analysis in Fisheries Ecology. PLOS ONE. 2014;9(6): e100195. https://doi.org/10.1371/journal.pone.0100195.
36. Russo T, Parisi A, Cataudella S. New insights in interpolating fishing tracks from VMS data for different métiers. Fish Res. 2011;108(1):184–94. https://doi.org/10.1016/j.fishres.2010.12.020.

37. Zhao Z, Chen J, Shi Y, Hong F, Jiang G, Huang H, et al. HiTrip: Historical trajectory interpolation for trawlers via deep learning on multi-source data. Ocean Eng. 2024;292: 116588.
38. Magnussen BB, Bläser N, Lu H. DAISTIN: A Data-Driven AIS Trajectory Interpolation Method. In: Proceedings of the 18th International Symposium on Spatial and Temporal Data; 2023. p. 75–84.
39. Pallotta G, Vespe M, Bryan K. Vessel Pattern Knowledge Discovery from AIS Data: A Framework for Anomaly Detection and Route Prediction. Entropy. 2013;15(6):2218–45.
40. Pallotta G, Horn S, Braca P, Bryan K. Context-enhanced vessel prediction based on Ornstein-Uhlenbeck processes using historical AIS traffic patterns: Real-world experimental results. In: 17th International Conference on Information Fusion (FUSION); 2014. p. 1–7.
41. Mazzarella F, Arguedas VF, Vespe M. Knowledge-based vessel position prediction using historical AIS data. in, sensor data fusion: trends solutions. Applications (SDF). 2015;2015:1–6.
42. Hexeberg S, Flaten AL, Eriksen BOH, Brekke EF. AIS-based vessel trajectory prediction. In: 2017 20th International Conference on Information Fusion (Fusion); 2017. p. 1–8.
43. Emmanuel T, Maupong T, Mpoeleng D, Semong T, Mphago B, Tabona O. A survey on missing data in machine learning. J Big Data. 2021;8(1):1–37.
44. Xu Y, Bazarjani A, Chi Hg, Choi C, Fu Y. Uncovering the missing pattern: Unified framework towards trajectory imputation and prediction. In: Proceedings of the IEEE/CVF Conference on Computer Vision and Pattern Recognition; 2023. p. 9632–9643.
45. Jia C, Ma J. Conditional temporal GAN for intent-aware vessel trajectory prediction in the precautionary area. Eng Appl Artif Intell. 2023;126: 106776.
46. Huang L, Huang J, Li H, Cui J. Robust spatial temporal imputation based on spatio-temporal generative adversarial nets. Knowl-Based Syst. 2023;279: 110919.
47. Xie H, Xue F, Wang X. Generative Models for Missing Data. Cham: Springer; 2024.
48. Ma J, Cheng JC, Jiang F, Chen W, Wang M, Zhai C. A bi-directional missing data imputation scheme based on LSTM and transfer learning for building energy data. Energy Build. 2020;216: 109941.
49. Yang CH, Wu CH, Shao JC, Wang YC, Hsieh CM. AIS-based intelligent vessel trajectory prediction using Bi-LSTM. IEEE Access. 2022;10:24302–15. https://doi.org/10.1109/ACCESS.2022.3154812.
50. Zhang Y, Han Z, Zhou X, Zhang L, Wang L, Zhen E, et al. PESO: a Seq2Seq-based vessel trajectory prediction method with parallel encoders and ship-oriented decoder. Appl Sci. 2023;13(7):4307.
51. Galdelli A, Armelloni EN, Ferrà C, Pulcinella J, Scarcella G, Tassetti AN.: R4AIS: an R workflow to process AIS data for fishery. Zenodo. Available from: https://doi.org/10.5281/zenodo.4761890.
52. Patrikar J, Moon B, Oh J, Scherer S. Predicting like a pilot: Dataset and method to predict socially-aware aircraft trajectories in non-towered terminal airspace. In: 2022 International Conference on Robotics and Automation (ICRA). IEEE; 2022. p. 2525–2531.
53. Pedregosa F, Varoquaux G, Gramfort A, Michel V, Thirion B, Grisel O, et al. Scikit-learn: machine learning in Python. J Machine Learn Res. 2011;12:2825–30.
54. Park SH, Lee G, Seo J, Bhat M, Kang M, Francis J, et al. Diverse and admissible trajectory forecasting through multimodal context understanding. Cham: Springer; 2020.
55. Li L, Jamieson K, DeSalvo G, Rostamizadeh A, Talwalkar A. Hyperband: a novel bandit-based approach to hyperparameter optimization. J Mach Learn Res. 2018;18(185):1–52.

Publisher's Note